Slov Vet Res 2023; 60 (Suppl 25): 133–47
DOI 10.26873/SVR-1573-2022

Original Research Article
Veterinary Medicine and The One Health Concept

ANTI-CANCER ACTIVITY OF GRAVIOLA (*Annona muricata*) LEAVES EXTRACT ON INDUCED BREAST CANCER IN RATS' MODEL

Areej I. Salem[1]*, Hosny Abd El-Fadil[1], Nagaah Al-Sayed[1], Ahmed S. Alazzouni[2], Sameh El-Nabtity[1]

[1]Department of Pharmacology, Faculty of Veterinary Medicine, Zagazig University, [2]Department of Zoology, Faculty of Science, Helwan University, Egypt

*Corresponding author, E-mail: areejibrahim3@gmail.com

Abstract: Breast cancer is the most frequent type of invasive cancer in women. However, chemotherapy affects all cells that grow and divide quickly in the body, including cancer and normal cells. On the other hand, Graviola is commonly used as a source of food and has a wide range of bioactive components. In this study, out of 50 albino rats, breast cancer was induced in 40 rats using 7,12-dimethylbenanthracene (DMBA). These rats were subjected to the treatment using Graviola leaves ethanolic extract (GLEE) and 5-Fluorouracil (5-FU) to evaluate the anti-carcinogenic activity and the immunohistochemical changes. A single oral dose of DMBA led to the induction of rats' breast cancer. Induced mammary tumors were diagnosed, and all were malignant without any benign tumor. Among the malignant tumors, non-invasive, invasive, mixed (invasive and non-invasive), and unclassified malignant tumors were detected. The immunohistochemical analysis showed that estrogen and progesterone receptors revealed negative nuclear expression. However, HER2 receptors score was +3, and Ki-67 revealed 85-90% nuclear stainability, denoting a very high proliferative index. The morphometric analysis revealed that staining reactivities of HER2 and Ki-67 were 60.66 and 89.84%, respectively, and were significantly higher than ER (15.24 %) and PR (15.68%). Genetic studies revealed marked upregulation of P53 with GLEE more than 5-FU while Bcl2 showed down regulation with GLEE more than 5-FU. The quantitative analysis of GLEE phytochemical constituents showed the presence of some bioactive chemical compounds that exhibit many therapeutic activities. Therefore, GLEE improved histological appearance of DMBA induced breast cancer in female rats. Therefore, GLEE could be a promising natural alternative to chemotherapy agents as a potent anticancer.

Key words: breast cancer; graviola; phytochemical; DMBA; 5-Flurouracil; P53; Bcl2

Introduction

Breast cancer is considered one of the most frequent malignancies in women taking into consideration one-quarter of all malignancies diagnosed in women and could be a heterogeneous illness on the molecular level (1). This cancer is developed in breast tissues, including lobules and ducts. The worldwide deaths in women related to cancers represent a worldwide burden. Globally, breast cancer incidence has been steadily increasing over the last few decades (2). Breast cancer was assessed to be 30% of recently analyzed cancer cases and about 15% of cancer-related deaths in women (3).

Breast cancer can be categorized into non-invasive or invasive. The surrogate intrinsic subtypes are dependent on key proteins histological and immunohistochemical examination: progesterone receptor (PR), estrogen receptor (ER), the proliferation marker Ki67, as well as human epidermal growth factor receptor 2 (HER2) (4). The strongest predictors in detecting and determining the risk for metastasis are the tumor diameter, axillary lymph nodes metastasis, histological grade, HER2

Received: 8 September 2022
Accepted for publication: 25 October 2022

status and hormone receptors, beside the Ki-67 proliferation index (5).

Bioactive compounds derived from natural products have recently gained considerable attention due to their efficacy in treating inflammatory diseases such as cancer. Earlier studies, including epidemiological, preclinical, and clinical studies, have suggested that consuming polyphenols, which are abundant in fruits and vegetables, may help to limit the advancement of numerous diseases, including cancer (6). In addition, dietary phytochemicals have numerous inherent benefits over manufactured substances because of their known safety, low cost, and oral bioavailability. Many researchers are studying plant-derived drug modes of action at the molecular, cellular, as well as tissue levels (7).

Graviola (*Annona muricata*) is a plant in the *Annonaceae* family that is both a source of nutrition and an indigenous medicinal herb. It has been proven to have a wide range of bioactivities, including anti-cancer properties (8).

All aerial and subterranean parts of Graviola, such as leaves, fruits, seeds, as well as roots, have all been applied in traditional medicine (9). Therefore, several studies on various parts of Graviola have demonstrated the presence of different phytochemical substances, including cyclopeptides and essential oils (10), flavonoltriglycosides (11), phenolics (12), and alkaloids (13). Hence, phytochemical studies indicated that the Annonaceae family's major constituents were acetogenins. Graviola's phenolic compounds have been shown to recover free radicals from human breast cancer cells (14). The plant has long been used to produce chemically active metabolites (15). Extensive anti-cancer studies have been conducted on Graviola due to its ethnomedicinal applications against tumors and cancer. Graviola induced apoptosis, necrosis, and inhibition of proliferation (16) on a diversity of cancer cell lines, in between breast, colorectal, lung, prostate, pancreatic, leukemia, hepatic, renal, cervical, and ovarian cancers (17).

5-Fluorouracil (5-FU) is an antineoplastic antimetabolite drug effective in the palliative management of carcinomas of different organs, and treatment of head, and neck carcinomas (18). Anti-cancer drugs are frequently given systemically, affecting tumor cells as well as all other body organs, resulting in increased toxicity in normal cells.

A tumor suppressor gene called wild type p53 is essential for preserving a cell's genomic integrity because it stops cells with damaged DNA from proliferation. The most frequent genetic flaws seen in clinical cancer are p53 mutations and deletions. Immunohistochemistry has been used to identify significant quantities of stable, frequently mutant, p53 protein in the cells of about 40% of breast carcinomas. Similar cells lacking p53 activity continue to proliferate, perpetuating potentially cancerous alterations, while cells with functional p53 perish via apoptosis. In addition to possibly serving as a predictor of a tumor's biological aggressiveness and potential response to treatment, the restoration of normal p53 function is already one of the main objectives of cancer therapy (19).

The BCL2 family of proteins is essential for controlling apoptosis. New members of the BCL2 gene family were found to express themselves differently in many diverse types of cancer (20).

A set of proteins known as caspases conduct the evolutionarily conserved apoptosis mechanism. Caspases are cysteine proteases that break down their substrates after an Asp residue. They are created as latent zymogenes and are then activated by proteolytic cleavage; the BCL2 family proteins primarily control this process (20).

Consequently, this study conducted to evaluate the anticancer activity of Graviola leaves ethanolic extract (GLEE) in comparison with the commercial therapeutic drug (5-FU) on 7,12-dimethylbenz[a] anthracene (DMBA)–induced breast cancer in rats by investigating the histological and immunohistochemical changes.

Material and methods

Graviola leaves preparation and extraction

Fresh Graviola leaves were obtained from the Faculty of Agriculture, Zagazig University, Egypt. The leaves were harvested, rinsed with tap water, and air-dried for four weeks at 25 °C. A milling machine was used to grind the plant samples into a homogeneous powder. The plant tissue homogenization method was used to extract equal amounts (350 g) of powdered leaves using 96% ethanol for three days (21). The prepared extract was concentrated by a rotary evaporator then stored at -20 °C for further use.

Phytochemical screening of Graviola extract

Sample derivatizations:

The samples were extracted and resuspended in 50 µL of N, O-bis (trimethylsilyl) trifluoroacetamide (BSTFA) incubated in a Dry Block Heater at 70 °C for 30 min.

Gas chromatography–mass spectrometry analysis (GC-MS):

The GC-MS system (Agilent Technologies) was equipped with gas chromatograph (7890B) and mass spectrometer detector (5977A) at Central Laboratories Network, National Research Centre, Cairo, Egypt. The GC was outfitted with an HP-5MS column that measured 30 m and had an internal diameter and film thickness of 0.25 mm. The following temperature program was used for the analyses, with hydrogen serving as the carrier gas, flowing at a rate of 1.0 ml/min at a splitless injection volume of 1 l: 50 °C for one minute, followed by a 20-minute hold at 300 °C after rising 10 °C/min. At 250 °C, the injector and detector were maintained. By employing a spectral range of m/z 30-700 and a solvent delay of 9 min, mass spectra were produced using electron ionization (EI) at 70 eV. The mass temperature was 230 °C and Quad 150 °C. Identification of different constituents was determined by comparing the spectrum fragmentation pattern with those stored in Wiley and NIST Mass Spectral Library data.

Experimental animals

This study was performed on fifty mature female albino rats weighing 100 - 120 g that were purchased from laboratory animal house at the Faculty of Veterinary Medicine, Zagazig University. Throughout the trial, the animals were housed at 23 ± 2 °C with a 12-hour light/dark cycle, and they had free access to standard food and water. Attempts were taken to reduce the pain and suffering of the animals during the research. They were removed from the trial and euthanized under deep anesthesia if they displayed aberrant symptoms. The ethical guidelines of dealing with laboratory animals were observed throughout the investigation, and this protocol was evaluated and approved by the ZU-IACUC committee with the permission number ZU-IACUC/2/F/63/2020, Zagazig University, Egypt.

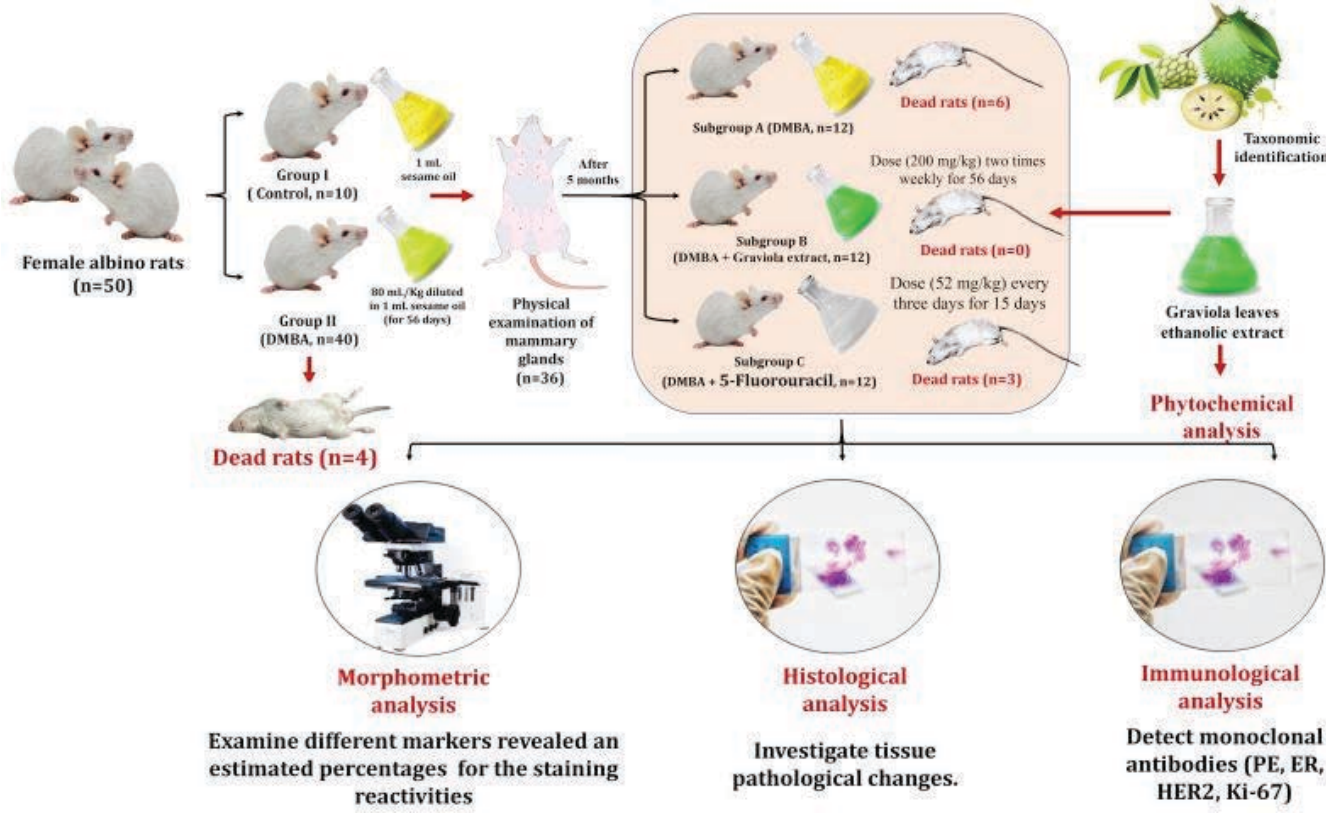

Figure 1: Experimental design of Breast cancer induction using DMBA in albino rats.

Experimental design

As shown in Fig. 1, after one week of acclimation, 50 female albino rats were divided into two experimental groups. Group I (control, n = 10) was given 1 mL sesame oil orally, while Group II (DMBA, n = 40) was given a single dose of DMBA (80 mg/kg, diluted in 1 mL sesame oil) by stomach tube (p.o.). Weekly physical examinations were conducted. Inspection, touching, and palpation were used to check each rat's six pairs of mammary glands. After 5 months and the confirmation of the tumor incidence by palpation and excluding the mortality ratio of investigated rats, as shown in Fig. 1, Group II was divided into three subgroups; subgroup A (DMBA, n = 12) is considered a positive control group, and subgroup B (DMBA + Graviola extract, n = 12) administrated GLEE to DMBA induced breast cancer in rats at a dose (200 mg/kg) two times weekly (p.o.) for eight weeks according to (22), subgroup C (DMBA + 5-FU, n = 12), administrated 5-FU at a dose (52 mg/kg) (i.p.) every three days (day 0, 3, 6, 9, 12, and 15). The applied dose was according to the previous method (23).

Rats of subgroup C were sacrificed at the 16th day post-administration of 5-FU, while rats of subgroup A and subgroup B were sacrificed at 7 months post-administration of DMBA, and animals were sacrificed by CO2 asphyxiation. And a section of the tumors were fixed in buffered formalin.

Histopathological and immunohistochemical analysis.

The formalin-preserved rat's mammary gland tissue specimens were impregnated with molten paraffin wax, then embedded and blocked out. The obtained paraffin sections were then stained with Hematoxylin and Eosin (H&E) based on the described method (24). Stained sections were examined for histopathological changes.

ER, PR and HER2 were detected by a specific primary monoclonal antibody. Paraffin was removed from the investigated sections (4 µm) using xylene and slowly rehydrated using ethanol. Antigen retrieval was performed using microwave in 10 mM citric acid monohydrate at 900 W for 1 × 5 min and at 600 W for 3 × 5 min. Treatment with H_2O_2 (0.5%) blocked the endogenous peroxidase activity. The prepared slides were kept overnight at 4 °C with the primary antibodies at appropriate dilutions. The negative controls were prepared by the same procedures without the overnight incubation; however, performed in PBS diluent without antibody.

For PR, the sections were subjected to dual colorimetric immunohistochemical (Envision G/2 Doublestain, Dako). However, For ER, the reaction was visualized using the Elite ABC Kit (Vectastain, CA, USA). The result was evaluated as the proportion of positively stained tumor cells (0–100%). The investigated samples were considered as positive for PR and ER when ≥1% of the tumor cells exhibited positive nuclear staining (25). For PR dual staining tumors, ≥1% Diaminobenzidine-stained nuclei or ≥1% Perm Red-stained cytoplasm were considered positive.

For HER2, the Envision kit (Dako, Denmark) was applied (24). HER2 was evaluated based on the intensity and percentage of positive cells on a scale of 0 to +3. The result was reported as negative (0) if no staining or membrane staining in less than 10% of invasive tumor cells was detected, or negative (+1) if faint/barely perceptive membrane staining was detected in more than 10% of invasive tumor cells. However, the result was considered positive (+2) when weak to moderate complete membrane staining in more than 10% tumor cells or <30% with strong complete membrane staining, or positive (+3) if strong complete membrane staining in >30% invasive tumor cells was detected (26). For Ki-67, tissue samples were considered positive for the tumor when ≥14% of the tumor cells exhibited positively stained nuclei (27). The Ki-67 index is defined as the percentage of the total number of tumor cells with nuclear staining (28). Immuno-stained cells were explored in different groups according to their numbers and nuclear staining intensity using the IMAGE J software analysis.

Morphometric analysis

Morphometric analysis was digitized using Olympus digital camera (Olympus LC20- Japan) installed on Olympus microscope (Olympus BX-50, Tokyo, Japan) with 1/2X photo adaptor, using 40X objective. The software Video Test Morphology 5.2 (Russia), which has a dedicated built-in method for immunohistostaining analysis, was used to evaluate the results photos. Average grayscale was used to express the immunoreactive

intensity. High values were <160, and medium values ranged from 160 to 170, and low values ranged from170 to180 (29).

Gene expression and reverse transcription polymerase chain reaction (RT PCR).

RT-PCR analysis was digitized using *Rotorgene RT- PCR system* and Qiagen RNA extraction/ BioRad syber green PCR MMX kit. Analyses were carried out using DMSO as the solvent. Primers used in this study were presented in Table 1.

Results

Phytochemical analysis of ethanolic leaves extract of Graviola

As shown in Fig. 2, the phytochemical analysis by GC-MS analysis of GLEE revealed the presence of different bioactive compounds. The details of the GC-MS analysis of the extracts are listed in Table 2.

Table 1: Primers used in the present study

Target	Nucleotide sequence
Bcl2	F: 5'-ATCGCCCTGTGGATGACTGAGT-3' R: 5'-GCCAGGAGAAATCAAACAGAGGC-3'
Casp3	F: 5'-TTCATTATTCAGGCCTGCCGAGG-3' R: 5'-TTCTGACAGGCCATGTCATCCTCA-3'

Target	Nucleotide sequence
P53	F: 5'-CCTCAGCATCTTATCCGAGTGG-3' R: 5'-TGGATGGTGGTACAGTCAGAGC -3'
β-actin	F:5'-ATCGTGGGGCGCCCCAGGCAC-3' R:5'-CTCCTTAATGTCACGCACGATTTC-3'

Table 2: Phyto-components obtained from the Annona muricata ethanolic leaves extract using GC-MS

Peak	RT	Name	Formula	Area	Area Sum %
1	12.812	D-(-)-Lactic acid, trimethylsilyl ether	C6H14O3Si	29550.77	0.24
2	13.161	Propanoic acid, 3-(trimethylsilyl)-	C6H14O2Si	204646.07	1.63
3	16.216	Butanoic acid, 4-[(trimethylsilyl)oxy]-, trimethylsilyl ester (CAS)	C10H24O3Si2	72449.35	0.58
4	20.502	3-(Bistrifluoromethylamino-oxy)norbornylene	C9H9F6NO	69062.06	0.55
5	20.817	Arachidonic acid, TMS derivative	C23H40O2Si	98415.71	0.78
6	21.738	Germacrene D	C15H24	54323.81	0.43
7	23.134	2-Hydroxyisocaproic acid, TMS derivative	C9H20O3Si	47663.68	0.38
8	23.815	Aromandendrene	C15H24	70628.83	0.56
9	24.159	9,12-Octadecadiynoic acid, trimethylsilyl ester	C21H38O2Si	89930.65	0.72
10	24.433	5-Hydroxymethyl-2,2,5-trimethyl-1,3-dioxane, TMS derivative	C11H24O3Si	233462.98	1.86
11	24.748	Methyl .alpha.-Arabinofuranoside, 3TMS derivative	C15H30O5Si3	359310.9	2.86
12	24.891	D-(-)-Ribofuranose, tetrakis(trimethylsilyl) ether (isomer 1)	C17H42O5Si4	512373.99	4.08
13	25.257	1,3-Dihydroxyacetone dimer, 4TMS derivative	C18H46O6Si4	1331645.5	10.6
14	25.532	D-(-)-Lyxofuranose, tetrakis(trimethylsilyl) ether	C17H42O5Si4	1121679.3	8.93
15	25.652	L-(-)-Sorbofuranose, pentakis(trimethylsilyl) ether	C21H52O6Si5	798000.22	6.35
16	26.012	D-(-)-Fructopyranose, pentakis(trimethylsilyl) ether (isomer 1)	C21H52O6Si5	732986.99	5.83
17	26.178	D-Psicofuranose, pentakis(trimethylsilyl) ether (isomer 1)	C21H52O6Si5	408524.64	3.25
18	26.287	D-Lyxose, 4TMS derivative	C17H42O5Si4	127728.01	1.02
19	26.459	D-Glucopyranose, 5TMS derivative	C21H52O6Si5	85661.53	0.68
20	26.791	beta.-D-(+)-Talopyranose, 5TMS derivative	C21H52O6Si5	519150.01	4.13
21	27.031	beta.-D-(+)-Xylopyranose, 4TMS derivative	C17H42O5Si4	555103.42	4.42
22	27.363	D-Arabinopyranose, 4TMS derivative (isomer 2)	C17H42O5Si4	1020398.9	8.12
23	27.695	Glucose, 5TMS derivative	C21H52O6Si5	895722.74	7.13
24	28.462	Scyllo-Inositol, 6TMS derivative	C24H60O6Si6	336907.67	2.68
25	28.627	Myo-Inositol, 6TMS derivative	C24H60O6Si6	1069880.3	8.52
26	28.885	9,12,15-Octadecatrienoic acid, methyl ester, (Z,Z,Z)-	C19H32O2	281593.1	2.24
27	29.108	Phosphonic acid, dioctadecyl ester	C36H75O4P	421307.1	3.35
28	29.926	Methyl galactoside (1R,2R,3S,4S,5R)-, 4TMS derivative	C19H46O6Si4	51776.68	0.41
29	31.088	1H-3a,7-Methanoazulene, octahydro-1,4,9,9-tetramethyl-	C15H26	53446.93	0.43
30	32.061	1,2-Benzenedicaboxylic acid, bis(2-ethylhexyl) ester	C24H38O4	38999.18	0.31
31	32.427	Adamantane-1-carboxamide, N-[2-(3,4-dimethylphenoxy)ethyl]-	C21H29NO2	36219.71	0.29
32	33.148	arachidonic acid tert-butyldimethylsilyl ester	C26H46O2Si	43174.55	0.34
33	33.875	Pinellic acid, 2TMS derivative	C13H28O4Si2	31202.22	0.25
34	36.055	dl-.alpha.-Tocopherol	C29H50O2	149904.45	1.19
35	36.633	(E)-5,10-secocholest-1(10)-en-3,5-dione	C27H44O2	98489.91	0.78
36	36.827	Stigmasterol	C29H48O	64887.82	0.52
37	36.93	3-Amino-2-carbomethoxy-4,4,6,6-tetramethyl-4,6-dihydro-5H-thieno[2,3-c]pyrrole-5-yloxyl radical	C12H17N2O3S	106029.52	0.84
38	37.182	gamma.-Sitosterol	C29H50O	277184.14	2.21
39	37.342	Cholest-5-en-3-ol (3β)-, 9-octadecenoate, (Z)-	C12H17N2O3S	65124.83	0.52

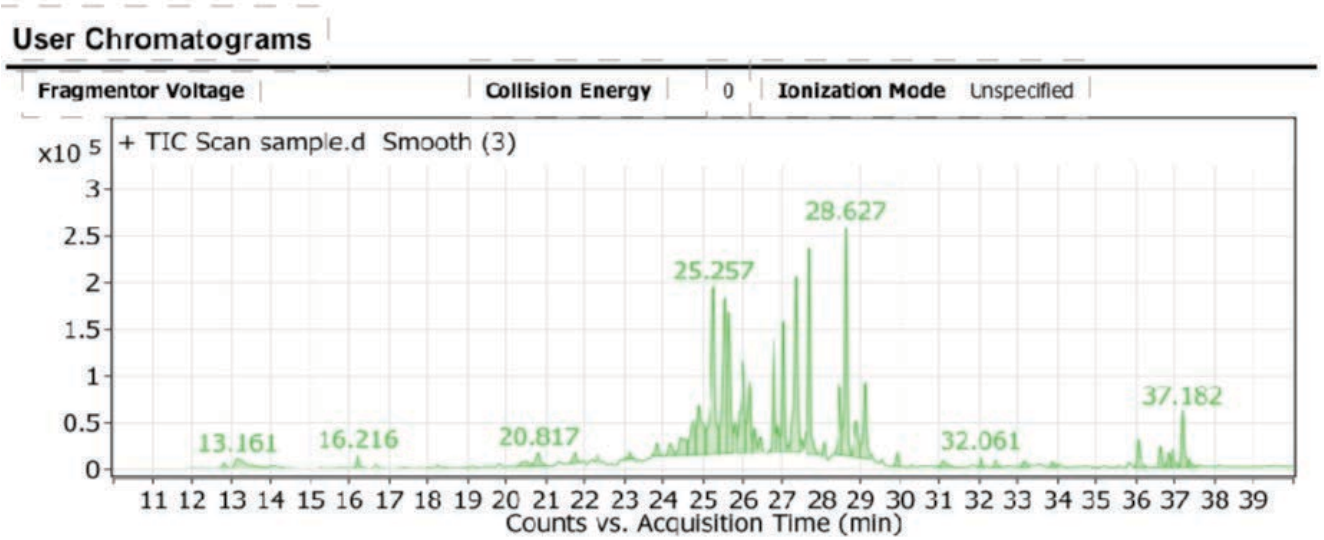

Figure 2: Phytochemical analysis by GC-MS analysis of GLEE

Histological Observations

Tumor induction and detection

Breast cancer was induced experimentally using a single oral dose of DMBA, as shown in Fig. 3.

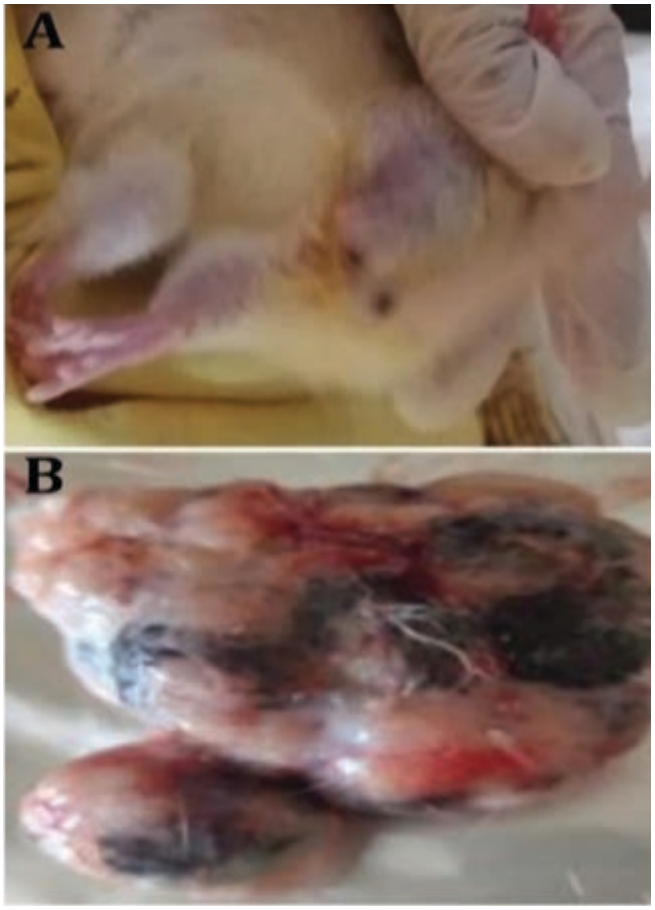

Figure 3: DMBA- induced breast cancer in albino rats

In our study, induced mammary tumors were diagnosed, in which 100% were malignant without any benign tumor. Among the malignant tumors, non-invasive, invasive, mixed invasive and non-invasive tumors, and unclassified malignant tumors were detected. Mammary gland of control adult female rats showed normal tissue architecture with normal secretory acini and ductules (Fig. 4A) that are lined with cuboidal or low columnar epithelial cells and surrounded by myoepithelial cells with loose connective tissue in between. As illustrated in Fig. 4B, the induction of rat's mammary gland tumor by DMBA shows sheets of tumor cells separated by tiny cystic gaps describe adenoid cystic carcinoma. Tumor cells appeared large, rounded with vesicular nuclei, enlarged nucleoli, and moderate mitotic activates in situ, and invasive papillary carcinoma was shown. Proliferating neoplastic cells were grouped in long finger-like extensions with a delicate fibrovascular core in the center and showed signs of malignancy (H&E). The scale bar is 50 µm. Figure 4C shows *in situ* and microinvasive papillary cancer. Proliferating neoplastic epithelial cells develop inward in the lumen to create finger-like papillary structures with little fibro-vascular core, which are restricted within the lobule by an intact basement membrane. A compact clump of malignant epithelial cells generated secondary projections (papillae). By breaching the foundation membrane, papillae from one lobule are visible entering the adjacent lobule (Fig. 4D).

As shown in Fig. 5, among all detected tumor types, invasive tubular adenocarcinoma (Fig.

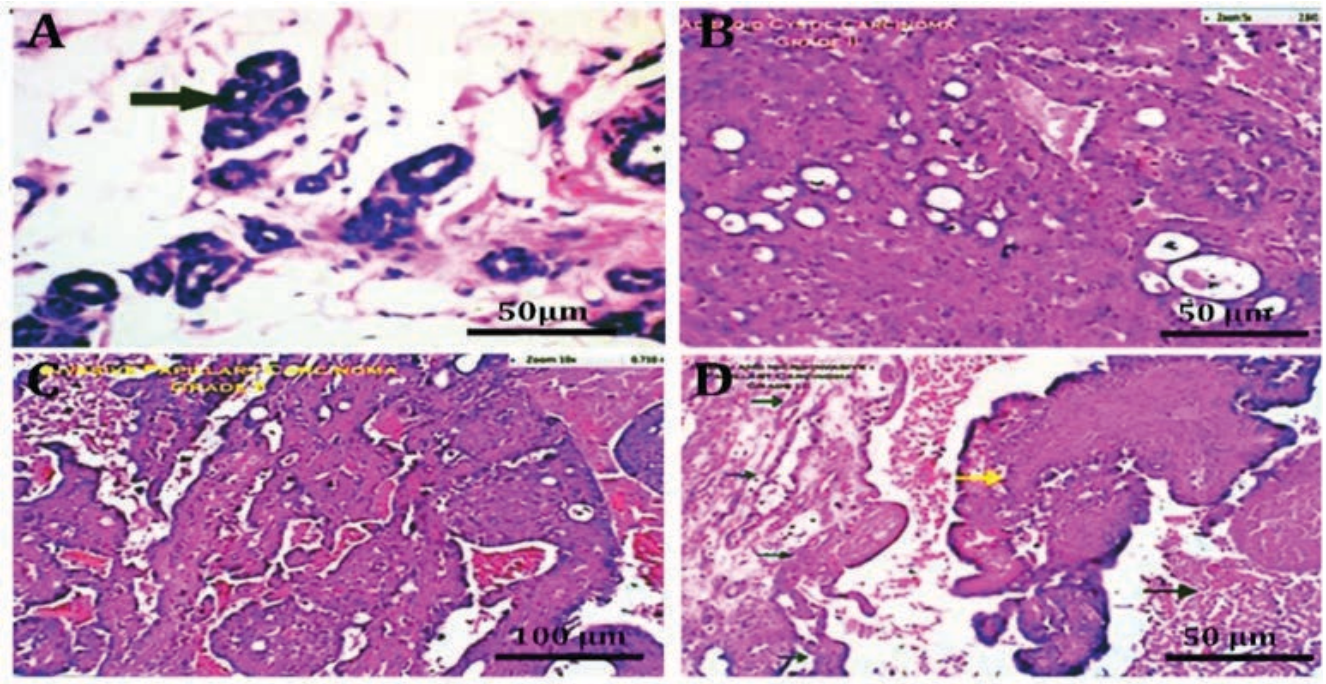

Figure 4: Mammary gland of control adult female rat (H&E) showing normal tissue architecture with normal acini (ar-row) and ductless with interlobular stroma inbetween (A). Mammary gland treated with DMBA showing ade-noid cystic carcinoma (B). induced rat's mammary gland tumor by (DMBA) showing invasive papillary carci-noma (C). Oncogenic epithelium cells that are proliferating, Secondary projections were generated by a com-pact cluster of neoplastic epithelial cells with moderate mitotic figures (3.210.04/hpf) (D)

5A) was characterized by clusters of ductal or alveolar structures proliferate, separated by a little quantity of connective tissue. The nuclei of the neoplastic cells ranged in size from circular to expanded oval, with conspicuous nucleoli. Mitotic figures were found in copious quantities (5.6 ± 0.24/hpf) and there was considerable tissue necrosis.

Solid cribriform carcinoma (in situ and invasive) was characterized by the appearance of the sieve is defined by proliferating neoplastic cells grouped in solid sheets with the frequent development of spherical or irregular-shaped secondary lumina of varying diameters. Neoplastic cells grew quickly and had a lot of pleomorphism. The neoplastic cells can be observed infecting the stroma around them (Fig. 5B).

Furthermore, as demonstrated in Fig. 5C, in situ and invasive comedocarcinoma was distinguished by dilated ductal structures lined by a multi-layered epithelium with necrotic material in the center. Desmoplastic reaction was seen in the stroma surrounding the separate ducts. Individual cancer cells were pleomorphic, with big hyperchromatic nuclei with conspicuous nucleoli.

Moreover, in situ and invasive ductal carcinoma (solid type), as shown in Fig. 5D**,** where mammary lobules were totally replaced by proliferating ductal cells, which completely obliterate and expand the main ducts with no evidence of microcystic or necrotic changes. Some tumor cells break the basement membrane, infiltrate and totally replace the adjacent tissue. Tumor cells were large hyperchromatic with the presence of moderate mitotic figures.

Furthermore, keratinized squamous cell carcinoma in rat mammary gland after DMBA induction, as shown in Fig. 5E**,** was detected and characterized by the presence of pathognomonic Epithelial Pearls showing invasive squamous cell carcinoma, characterized by many invasive malignant masses and columns invading the dermis and subcutaneous tissue. Tumor cells are hyperchromatic, pleomorphic with vesicular nuclei, and marked mitosis (Fig. 5F).

Immunohistochemical analysis

All examined tissue sections for estrogen receptors (Fig. 6A) progesterone receptors (Fig. 6B) revealed negative nuclear expression with a score of 0%. However, all examined tumor tissue sections treated by monoclonal antibodies against HER2 receptors revealed complete thick

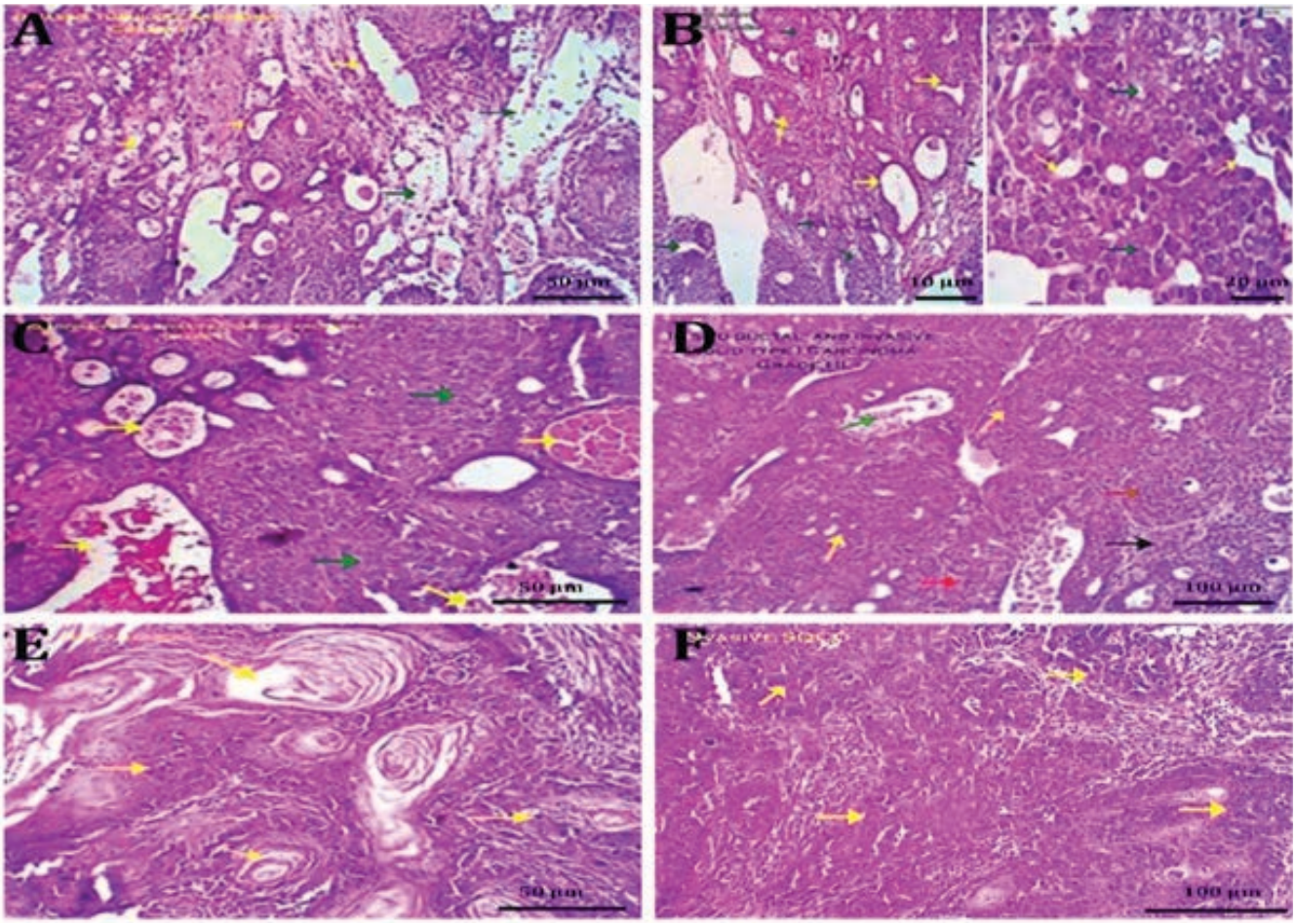

Figure 5: Experimentally induced rat's mammary gland tumor by DMBA (H&E) showing invasive tubular adenocarcinoma (A), in situ and invasive cribriform carcinoma (B), in situ and invasive comedo-carcinoma (C), in situ and invasive ductal carcinoma (D), keratinized squamous cell carcinoma (E), and invasive squamous cell carcinoma (F)

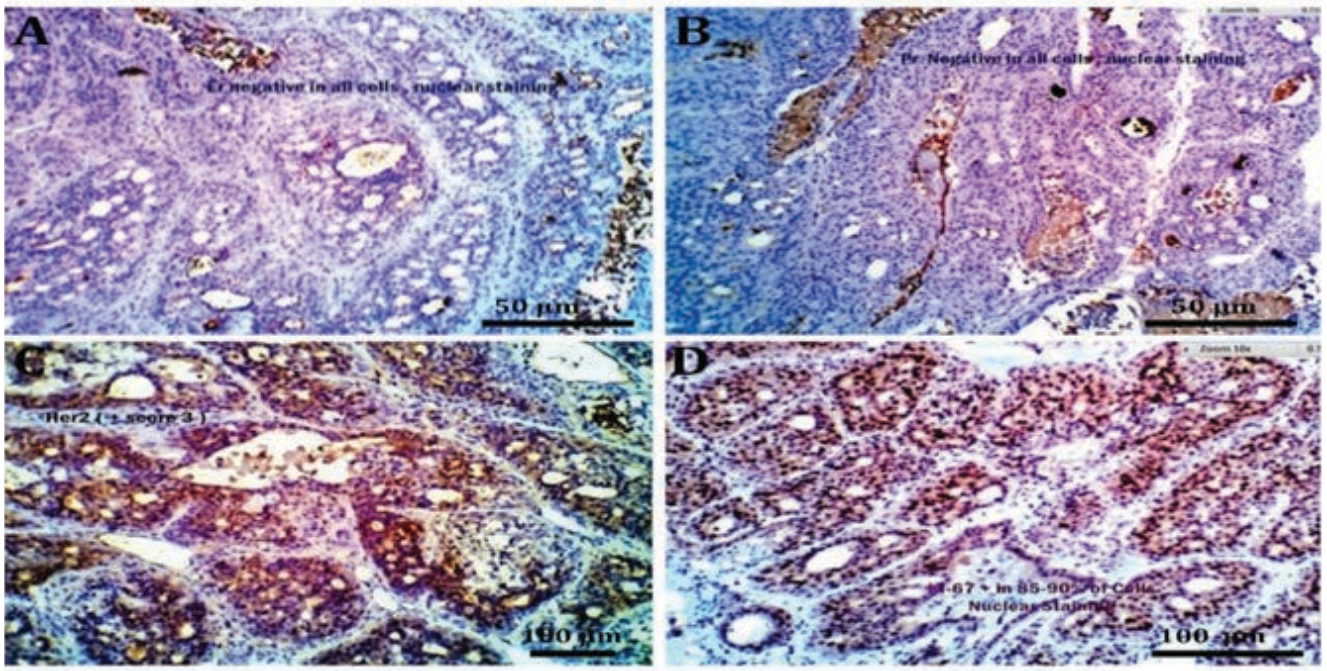

Figure 6: The immunohistochemical examination of induced rat's mammary gland tumor by DMBA showing negative nuclear expression of estrogen receptors in all tumor cells (A), a negative nuclear expression of progesterone receptors (B), HER2 immuno-stained cells with complete thick membrane staining reaction (C), and Ki-67 immuno-stained cells with high expression (D).

membrane staining reaction in more than 10% of the tumor cells with a score of +3 (Fig. 6C). Moreover, in breast cancer, Ki-67 identifies a high proliferative subset of patients. Treated tumor tissue sections by specific monoclonal antibodies against Ki-67 antigens revealed 85-90% nuclear stainability, denoting a very high proliferative index, as shown in Fig. 6D.

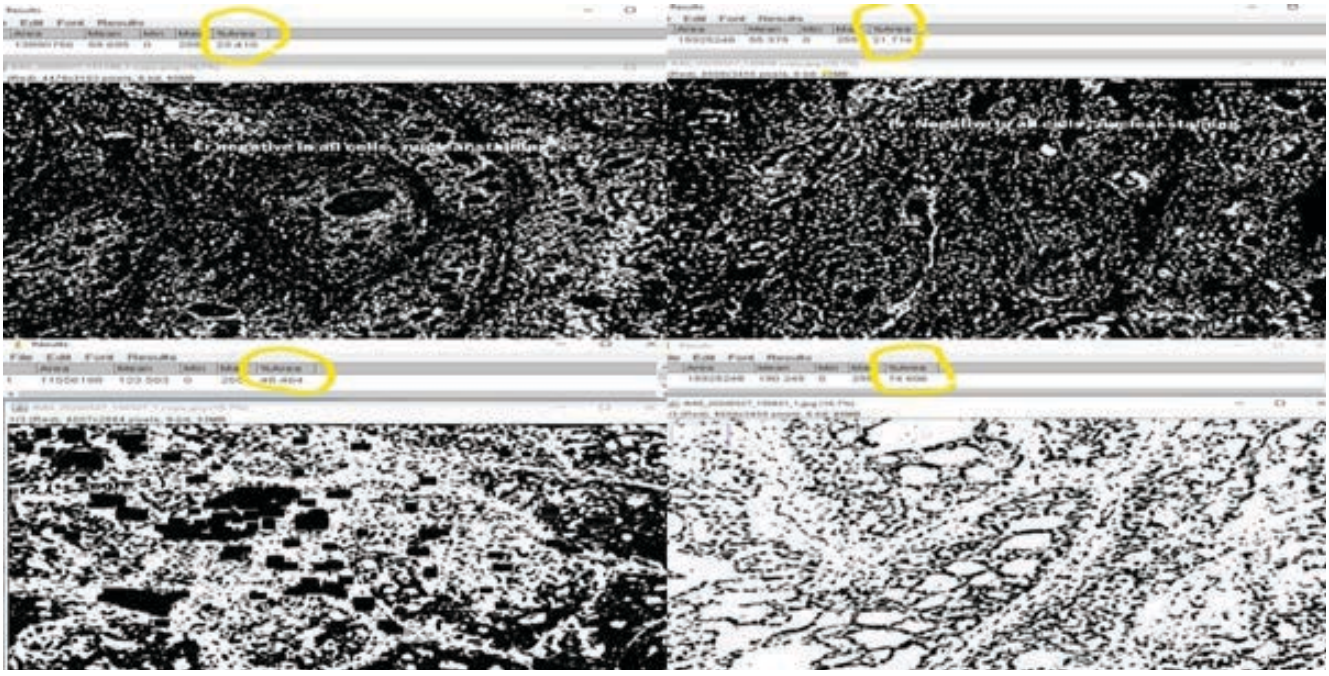

Figure 7: Morphometric analysis showing the morphometric analysis with an estimated percentage for the staining reac-tivates in the different used immunostaining markers.

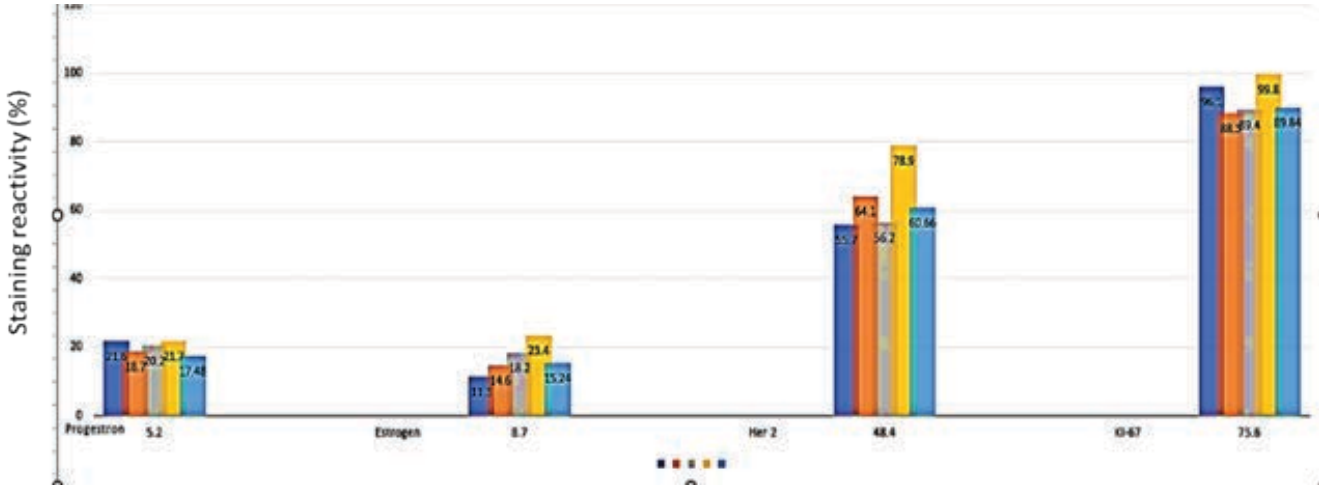

Figure 8: Illustrative statistical analysis chart for different immunostaining markers

Our obtained data of morphometric analysis (Fig. 7) revealed that staining reactivity of HER2 and Ki-67 was 60.66 and 89.84%, respectively, and were significantly (P <0.05) higher than ER and PR, which were estimated as 15.24 and 15.68%, respectively (Fig. 7B). Our statistical analysis showed that Ki-67 was significantly higher than HER2 (P 0.0023), ER (P <0.0001), and PR (P <0.0001). However, PR and ER were statistically insignificant (P 0.5956) (Fig. 8).

Treatment regimen using 5-FU

Based on our obtained results, we demonstrated three types of malignant tumors, including in situ ductal and comedo-carcinoma and invasive

tubular carcinoma. All of these tumoral tissues showed marked cytotoxic therapy response to 5-FU. Of those, 72-78 % of the tumor cells were necrotic; the remaining cells showed degenerative changes. Marked desmoplastic reactions were observed. The examined non-tumoral normal mammary tissue showed marked cytotoxic effect as most of the mammary acini were necrotic, as shown in Figure 9.

Treatment regimen with Graviola leaves extracts.

As shown in Fig. 10, the treatment using GLEE reduced tumor size compared to the positive control group. In the histological study, investigated sections of GLEE treated groups demonstrated a moderate to marked cytotoxic effect of the GLEE. Examined sections showed

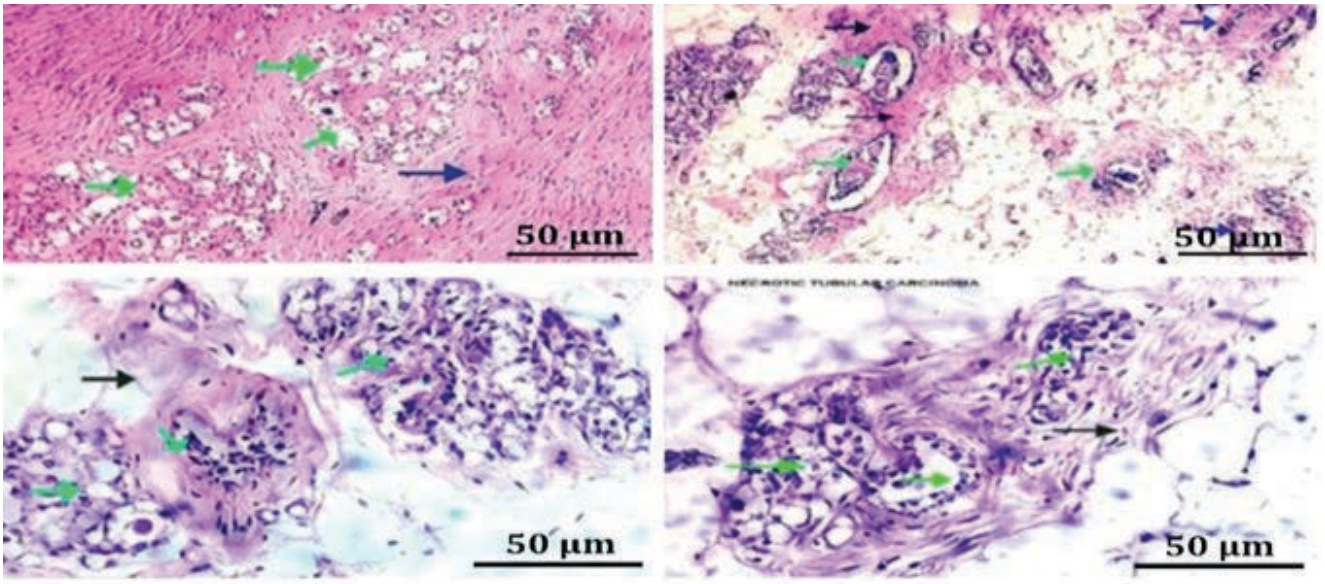

Figure 9: Induced rat's mammary gland tumor treated by 5-Fluorouracil, Of those, 72-78 % of the tumor cells were necrotic; the remaining cells showed degenerative changes. Marked desmoplastic reactions were observed. The examined non-tumoral normal mammary tissue showed marked cytotoxic effect as most of the mammary acini were necrotic

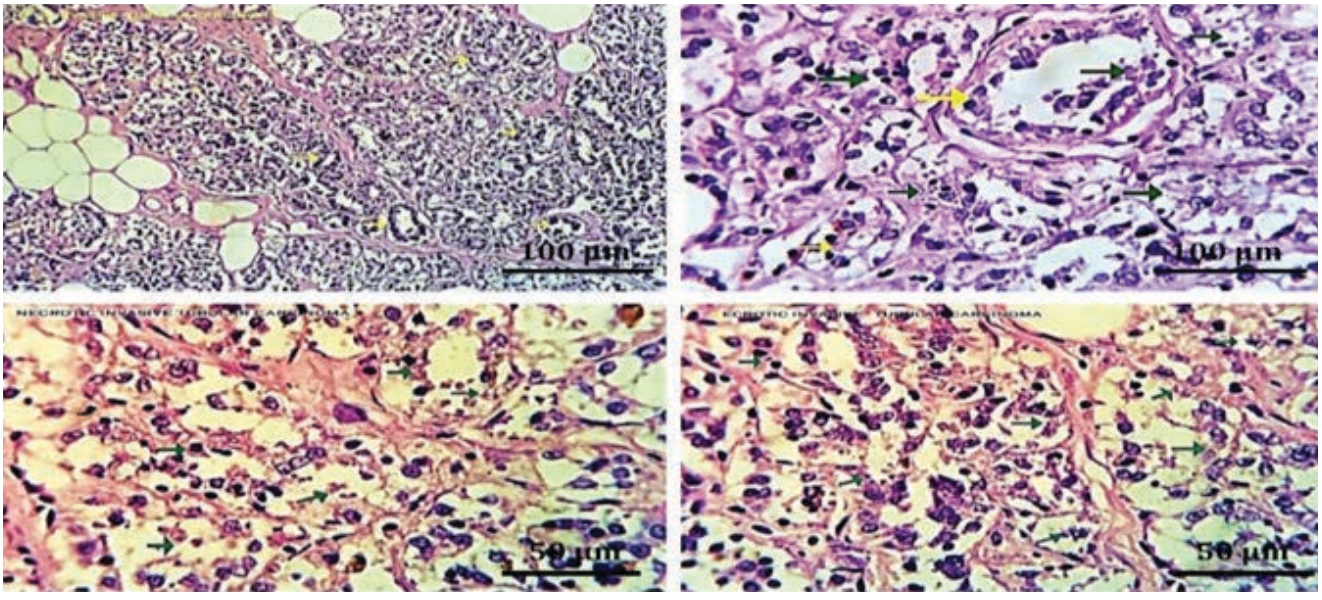

Figure 10: Induced rat's mammary gland tumor treated by Graviola L. extract, investigated sections of GLEE treated groups demonstrated a moderate to marked cytotoxic effect of the GLEE. Examined sections showed a marked cytotoxic effect of the plant extract, where a large number of the invasive tubular carcinoma cells were necrotic, as evidenced by pyknosis and karyorrhexis, and karyolysis of the tumor cells

a marked cytotoxic effect of the plant extract, where a large number of the invasive tubular carcinoma cells were necrotic, as evidenced by pyknosis and karyorrhexis, and karyolysis of the tumor cells. Moreover, a variable number of the invasive tumor cells showed apoptotic changes. The estimated therapeutic effect of the used extracts is ranged between 59-63%. The normal non-tumoral mammary tissue appeared healthy with an undetectable hazard effect of the used extracts.

Gene expression analysis

Genetic studies revealed marked up-regulation of P53 with GLEE more than 5-FU while Bcl2 showed down-regulation with GLEE more than 5-FU (Table 3).

Table 3: Genes expressions analysis of the experimental groups

Ser	Group	Fold Change	
		p53	Bcl2
1	DMBA group	4.01	0.51
2	DMBA + Graviola extract group	6.41	0.2
3	DMBA + 5-Fl Fluorouracil	3.28	0.35
4	Control group	1	1

Discussion

The most common invasive malignancy in women is breast carcinoma. Researchers have been working hard in recent years to discover a better treatment for breast carcinoma, and they are still working on it. It is also the second greatest cause of cancer-related death in women, after lung carcinoma (30).

In this study, DMBA was used for chemical induction of breast cancer which showed diverse types of breast cancer according to the histological subtypes (31).

In the present study, DMBA-induced breast cancer group revealed up regulation of P53, may be due to mutation of the p53 gene in DMBA-induced breast cancer cells led to cells lacking P53 function continue to proliferate, perpetuating potentially oncogenic mutations (32). Also, DMBA affect the microtubule dynamics through changing the expression of genes involved in cellular differentiation, proliferation/cell cycle regulation (33). The tumor incidence of our model was similar to other studies with the same chemical inductor (DMBA), which found tumor incidences of 82% (34), 92.3% (35), and 100% (36).

For the detection of Estrogen, Progesterone, and HER2 receptors in breast carcinoma cases for responsiveness to endocrine therapy in the management of breast cancer, immunohistochemistry is now a widely acknowledged approach. The immunohistochemistry investigation in our study demonstrated that the estrogen and progesterone receptors had negative nuclear expression. However, the HER2 receptors score was +3, and a nuclear stainability of between 85 and 90 percent on the Ki-67 test indicated a very high proliferative index. It has been shown that Ki-67 high expression enhances tumor growth in breast cancer rats by promoting breast cancer progression to higher histological grade in breast carcinoma rats (37). ER and PR were negatively correlated with HER2 overexpression (38). Also, the obtained results of HER2 in this study were similar to those reported before (26) where HER2 protein overexpression is found in tumors of around 25–30% of breast cancer patients, and this overexpression is associated with a poor clinical prognosis.

In our histological study, all of these tumoral tissues treated with 5-FU showed marked cytotoxic therapy response to 5-FU. Of those, 72-78 % of the tumor cells were necrotic; the remaining cells showed degenerative changes. Marked desmoplastic reactions were observed. The examined non-tumoral normal mammary tissue showed marked cytotoxic effect as most of the mammary acini were necrotic. By modifying cell death pathways, this medicine can decrease the spread of breast cancer in a variety of ways, including apoptosis. As a result, numerous treatment studies to overcome drug resistance caused by apoptosis modulation are now being done. 5-FU showed direct apoptotic action. 5-FU also has various modes of action, such as interfering with RNA processing and boosting p53 expression and our results in agreement with Prince *et al.* (18).

Natural products have been a target for cancer treatment because of their therapeutic properties for many years. In this study, the anti-cancer effect of the ethanolic leaf extract of Annona muricata was evaluated on induced HER2-positive breast cancer using DMBA in albino rats. Our study revealed that phytochemical analysis of the crude GLEE showed the presence of a complex

mixture of secondary metabolites that are found to have various therapeutic activities and GC-MS analysis showed bioactive compounds. Of these Arachidonic acid, Propanoic acid, Lactic acid, and Phytol. Our results agree with those of Ojezele *et al.* (39) and Magadi *et al.* (40). Beneficial anti-cancer activity of GLEE is due to its acetogenins contents (8). These *Annonaceous acetogenins* have the ability to block mitochondrial complex I, which can lead to cellular death by reducing intracellular ATP generation (41). Besides, Graviola extract improved glutathione S-transferase activity and glutathione levels, implying glutathione-dependent reactive oxygen species detoxification (ROS). Graviola's antioxidative properties can thus be related to its flavonoid concentration, which acts as a free radical scavenger and/or promotes the antioxidant system (40). Phytol also is known to have strong anticancer and immune-enhancing properties (42).

In the histological study, investigated sections of GLEE treated groups demonstrated that a large number of the invasive tubular carcinoma cells were necrotic as evidenced by pyknosis, karyorrhexis and Karryolysis of the tumor cells. Moreover, variable number of the invasive tumor cells showed apoptotic changes. Graviola, rather than apoptosis due to up-regulation of P53 and down regulation of Bcl2 in our genetic analysis, can destroy cancer cells by necrosis (43). Beside mitochondrial-dependent apoptotic pathway (44). This means that Gaviola's cytotoxic effect varies depending on the type of cancer cells, and that no single mechanism exists for all cancer cells.

Genetic analysis revealed upregulation of p53 and downregulation of Bcl2 indicating an increase in apoptotic index in graviola-treated group as compared to the carcinogen control and more than in 5-FU-treated group.

Apoptosis is induced as one of the most dramatic reactions to p53 activation. There are two main mechanisms through which apoptosis can occur: the intrinsic mitochondrial pathway and the extrinsic death receptor pathway (45). Bax and Bak oligomerization are induced in the mitochondria by p53, which also physically interacts with protective Bcl-XL and Bcl2 to counteract their antiapoptotic activities, disrupting the structure of the mitochondria (46). In this approach, it encourages the release of proteins that trigger apoptosis from the mitochondria, activating caspase-3 in the process. In the present study, Graviola treatment significantly decreased the Bcl2 expression whereas strong p53 expression was noted in breast cancer tissues.

Conclusions

In this study, we concluded that GLEE has several phytochemical components, which showed a moderate to marked anti-cancer effect on DMBA-induced breast cancer, and tumor cells showed apoptotic changes and up-regulation of P53 and down regulation of Bcl2 in comparison with traditional anticancer drug 5-FU. Moreover, it improved the histological appearance of DMBA-induced breast cancer in female rats. Therefore, Graviola could be a promising anticancer agent.

Acknowledgments

The authors gratefully acknowledge Dr. Hussein Abdel Baset (Botany Department, Zagazig University, Egypt) for his assistance in the identification of Graviola and his valuable assistance during the preparation of this manuscript.

A.I.S.: design of the experiment, animal work, methodology, data collection, writing the manuscript, and corresponding author. S.E. and A.S.A.: methodology and revision of the manuscript. H.A.E. and N.A.: methodology. The authors have read and approved the manuscript.

This research received no external funding.

The authors declare no conflict of interest.

References

1. Ferlay J, Soerjomataram I, Dikshit R, Eser S, Mathers C, Rebelo M, Parkin DM, Forman D, Bray F. Cancer incidence and mortality worldwide: Sources, methods and major patterns in GLOBOCAN 2012. Inter J Cancer 2014; 136: E359-E386. https://doi.org/10.1002/ijc.29210.

2. Jemal A, Siegel R, Xu J, Ward E. Cancer Statistics, 2010. CA: Cancer J Clin 2010; 60(5): 277–300. https://doi.org/10.3322/caac.20073.

3. Siegel RL, Miller KD, Jemal A. Cancer statistics, 2020. CA: Cancer J Clin 2020; 70(1): 7–30. https://doi.org/10.3322/caac.21590.

4. Harbeck N, Penault-Llorca F, Cortes J, Gnant M, Houssami N, Poortmans P, Ruddy K, Tsang J, Cardoso F. Breast cancer. Nat Rev Dis Primers 2019; 5(1). https://doi.org/10.1038/s41572-019-0111-2.

5. Masood S. Prognostic/Predictive Factors in Breast Cancer. Clin Lab Med 2005; 25(4): 809–25. https://doi.org/10.1016/j.cll.2005.08.012.

6. Ko JH, Sethi G, Um JY, Shanmugam MK, Arfuso F, Kumar AP, Bishayee A, Ahn KS (2017). The Role of Resveratrol in Cancer Therapy. Inter J Mol Sci 2017; 18(12): 2589. https://doi.org/10.3390/ijms18122589.

7. El-Beltagy AEFBM, Elsyyad HIH, Abdelaziz KK, Madany AS, Elghazaly MM. Therapeutic Role of *Annona muricata* Fruit and Bee Venom Against MNU-Induced Breast Cancer in Pregnant Rats and its Complications on the Ovaries. Breast Cancer 2021; 13: 431-445. https://doi.org/10.2147/BCTT.S306971.

8. Gnanga MNG, Assanhou AG, Ganfon H, Agbokponto EJ, Gbaguidi FA, Ahyi V. *Annona muricata* L. and *Annona squamosa* L. (Annonaceae): A review of their traditional uses and anti-cancer activities. J Pharm Phytochem 2021; 10(1): 40–1. https://doi.org/10.22271/phyto.2021.v10.i1a.13287.

9. Sun S, Liu J, Zhou N, Zhu W, Dou QP, Zhou K. Isolation of three new annonaceous acetogenins from Graviola fruit (*Annona muricata*) and their anti-proliferation on human prostate cancer cell PC-3. Bioorg Med Chem Lett 2016; 26(17): 4382–5. https://doi.org/10.1016/j.bmcl.2015.06.038

10. Kossouoh C, Moudachirou M, Adjakidje V, Chalchat JC, Figuérédo G. Essential Oil Chemical Composition of *Annona muricata* L. Leaves from Benin. J Essential Oil Res 2007; 19(4): 307–9. https://doi.org/10.1080/10412905.2007.9699288

11. Nawwar M, Ayoub N, Hussein S, Hashim A, El-Sharawy R, Wende K, Harms M, Lindequist U. Flavonol triglycoside and investigation of the antioxidant and cell stimulating activities of *Annona muricata* Linn. Arch Pharm Res 2012; 35(5): 761–7. https://doi.org/10.1007/s12272-012-0501-4.

12. Jiménez VM, Gruschwitz M, Schweiggert RM, Carle R, Esquivel P. Identification of phenolic compounds in soursop (Annona muricata) pulp by high-performance liquid chromatography with diode array and electrospray ionization mass spectrometric detection. Food Res Inter 2014; 65: 42–6. https://doi.org/10.1016/j.foodres.2014.05.051.

13. Yang C, Gundala SR, Mukkavilli R, Vangala S, Reid MD, Aneja R. Synergistic interactions among flavonoids and acetogenins in Graviola (*Annona muricata*) leaves confer protection against prostate cancer. Carcinogenesis 2015; 36(6): 656–65. https://doi.org/10.1093/carcin/bgv046

14. George VC, Kumar DRN, Rajkumar V, Suresh PK, Kumar RA. Quantitative Assessment of the Relative Antineoplastic Potential of the n-butanolic Leaf Extract of *Annona Muricata* Linn. in Normal and immortalized Human Cell Lines. Asian Pacific J Cancer Prev 2012; 13(2): 699–704. https://doi.org/10.7314/apjcp.2012.13.2.699.

15. Moghadamtousi ZS, Karimian H, Rouhollahi E, Paydar M, Fadaeinasab M, Abdul Kadir H. *Annona muricata* leaves induce G1 cell cycle arrest and apoptosis through mitochondria-mediated pathway in human HCT-116 and HT-29 colon cancer cells. J Ethnopharmacol 2014; 156: 277–89. https://doi.org/10.1016/j.jep.2014.08.011.

16. Moghadamtousi ZS, Rouhollahi E, Karimian H, Fadaeinasab M, Firoozinia M, Ameen Abdulla M, Abdul Kadir H. The chemopotential effect of *Annona muricata* leaves against azoxymethane-induced colonic aberrant crypt foci in rats and the apoptotic effect of Acetogenin Annomuricin E in HT-29 cells: a bioassay-guided approach. PloS One 2015; 10(4): e0122288–. https://doi.org/10.1371/journal.pone.0122288.

17. Rady I, Bloch MB, Chamcheu RCN, Banang Mbeumi S, Anwar MR, Mohamed H, Babatunde AS, Kuiate JR, Noubissi FK, El Sayed KA, Whitfield GK, Chamcheu JC. Anticancer Properties of Graviola (*Annona muricata*): A Comprehensive Mechanistic Review. Oxid Med Cellular Long 2018; 2018: 1826170. https://doi.org/10.1155/2018/1826170.

18. Prince GT, Cameron MC, Fathi R, Alkousakis T (2018). Topical 5-fluorouracil in dermatologic disease. Inter J Dermatol 2018; 57(10): 1259–64. https://doi.org/10.1111/ijd.14106.

19. Barnes DM, Camplejohn RS. P53, apoptosis, and breast cancer Review. J Mammary Gland Biol Neoplasia 1996; 1(2): 163-75. doi: 10.1007/BF02013640.

20. Zimmermann KC, Green DR. How cells die: apoptosis pathways, J Allergy Clin Immunol 2001; 108: S99-S103.

21. Tiwari AK, Saha SN, Yadav VP, et al. Extraction and characterization of pectin from orange peels. Inter J Biotechnol Biochem 2017; 13(1): 39–47.

22. Foong CP, Hamid RA. Evaluation of anti-inflammatory activities of ethanolic extract of *Annona muricata* leaves. Revista Brasileira de Farmacognosia. 2012; 22: 1301–7.

23. Yang H, Huang S, Wei Y, Cao S, Pi C, Feng T, Liang J, Zhao L, Ren G. Curcumin Enhances

the Anticancer Effect Of 5-fluorouracil against Gastric Cancer through Down-Regulation of COX-2 and NF- κB Signaling Pathways. Journal of Cancer 2017; 8(18): 3697–706.

24. Bancroft JD, Suvarna SK, Layton C, Bancroft JD, Suvarna SK, Layton C. Acknowledgments. In Bancroft's Theory and Practice of Histological Techniques 2019; (pp. ix–x). Elsevier. https://doi.org/10.1016/b978-0-7020-6864-5.04001-9.

25. Hammond MEH, Hayes DF, Wolff AC, Mangu PB, Temin S. American society of clinical oncology/college of american pathologists guideline recommendations for immunohistochemical testing of estrogen and progesterone receptors in breast cancer. J Oncol Pract 2010; 6(4): 195–7. https://doi.org/10.1200/JOP.777003.

26. Joensuu K, Leidenius M, Kero M, Andersson LC, Horwitz KB, Heikkilä P. ER, PR, HER2, Ki-67 and CK5 in Early and Late Relapsing Breast Cancer-Reduced CK5 Expression in Metastases. Breast Cancer: Basic Clin Res 2013; 7: 23–4. https://doi.org/10.4137/BCBCR.S10701

27. Cheang MCU, Chia SK, Voduc D, Gao D, Leung S, Snider J, Watson M, Davies S, Bernard PS, Parker JS, Perou CM, Ellis MJ, Nielsen TO. Ki67 index, HER2 status, and prognosis of patients with luminal B breast cancer. J National Cancer Inst 2009; 101(10): 736–50. https://doi.org/10.1093/jnci/djp082.

28. Urruticoechea A, Smith IE, Dowsett M. (2005). Proliferation Marker Ki-67 in Early Breast Cancer. J Clin Oncol 2005; 23(28): 7212–20. https://doi.org/10.1200/jco.2005.07.501

29. Cui W, Guo H, Cui H (2015). Vanadium toxicity in the thymic development. Oncotarget 2015; 6(30): 28661-28677. https://doi.org/10.18632/oncotarget.5798.

30. Bhatia R, Rawal RK. Coumarin Hybrids: Promising Scaffolds in the Treatment of Breast Cancer. Mini Rev Med Chem 2019; 19(17):1443–58

31. Feng M, Feng C, Yu Z, Fu Q, Ma Z, Wang F, Wang F, Yu L. Histopathological Alterations During Breast Carcinogenesis in a Rat Model Induced by 7,12-Dimethylbenz (a) Anthracene and EstrogenProgestogen Combinations. Int J Clin Exp Med 2015; 8(1): 346–57.

32. Weil S, Kito K, Miyoshi A, Matsumoto S, Kauzi A, Aramoto T, Abe Y, Ueda N. Incidence of p53 and ras gene mutations in DMBA-induced rat Leukemias. J Exper Clin Cancer Res 2002; 3(21): 1756–66.

33. Ma Z, Kim YM, Howard EW, Feng X, Kosanke SD, Yang S, Jiang Y, Parris AB, Cao X, Li S, Yang X. DMBA Promotes Erbb2mediated Carcinogenesis Via Erbb2 and Estrogen Receptor Pathway Activation and Genomic Instability. Oncol Rep 2018; 40(3): 1632-–40.

34. Bishayee A, Mandal A, Thoppil RJ, Darvesh AS, Bhatia D. Chemopreventive effect of a novel oleanane triterpenoid in a chemically induced rodent model of breast cancer. Inter J Cancer 2013; 133(5): 1054-1063. https://doi.org/10.1002/ijc.28108.

35. Alessandra-Perini J, Perini JA, Rodrigues-Baptista KC, de Moura RS, Junior AP, Dos Santos TA, Souza PJC, Nasciutti LE, Machado DE. Euterpe oleracea extract inhibits tumorigenesis effect of the chemical carcinogen DMBA in breast experimental cancer. BMC Comp Altern Med 2018; 18(1): 116. https://doi.org/10.1186/s12906-018-2183-z

36. Deepalakshmi K, Mirunalini S. Modulatory effect of Ganoderma lucidum on expression of xenobiotic enzymes, oxidant-antioxidant and hormonal status in 7,12-dimethylbenz(a)anthracene-induced mammary carcinoma in rats. Pharm Magaz 2013; 9(34): 167–75. https://doi.org/10.4103/0973-1296.111286.

37. Nishimura R, Osako T, Okumura Y, Hayashi M, Toyozumi Y, Arima N. Ki-67 as a prognostic marker according to breast cancer subtype and a predictor of recurrence time in primary breast cancer. Exp Therap Med 2010; 1(5): 747–54. https://doi.org/10.3892/etm.2010.133

38. Konecny G, Pauletti G, Pegram M, Untch M, Dandekar S, Aguilar Z, Wilson C, Rong HM, Bauerfeind I, Felber M, Wang HJ, Beryt M, Seshadri R, Hepp H, Slamon DJ. Quantitative Association Between HER-2/neu and Steroid Hormone Receptors in Hormone Receptor-Positive Primary Breast Cancer. JNCI J Nation Cancer Inst 2003; 95(2): 142-–53. https://doi.org/10.1093/jnci/95.2.142.

39. Ojezele OJ, Ojezele MO, Adeosun AM. Comparative phytochemistry and antioxidant activities of water and ethanol extract of *Annona muricata* Linn Leaf, seed and fruit. Adv Biol Res 2016; 10(4): 230–5. https://doi.org/10.5829/idosi.abr.2016.10.4.10514.

40. Magadi VP, Ravi V, Arpitha A, Litha Kumaraswamy K, Manjunath K. (2015). Evaluation of cytotoxicity of aqueous extract of Graviola leaves on squamous cell carcinoma cell-25 cell

lines by 3-(4,5-dimethylthiazol-2-Yl) -2,5-diphenyltetrazolium bromide assay and determination of percentage of cell inhibition at G2M phase of cell c. Contemporary Clin Dent 2015; 6(4): 529–33. https://doi.org/10.4103/0976-237X.169863.

41. de Pedro N, Cautain B, Melguizo A, Vicente F, Genilloud O, Peláez F, Tormo JR. (2012). Mitochondrial complex I inhibitors, acetogenins, induce HepG2 cell death through the induction of the complete apoptotic mitochondrial pathway. J Bioenerg Biomem 2012; 45: 153–64. https://doi.org/10.1007/s10863-012-9489-1.

42. Jeong SH. Inhibitory effect of Phytol on cellular senescence. Biomed Dermatol 2018; 2: 13. https://doi.org/10.1186/s41702-018-0025-8.

43. Torres MP, Rachagani S, Purohit V, Pandey P, Joshi S, Moore ED, Johansson SL, Singh PK, Ganti AK, Batra SK. Graviola: a novel promising natural-derived drug that inhibits tumorigenicity and metastasis of pancreatic cancer cells in vitro and in vivo through altering cell metabolism. Cancer Lett 2012; 323: 29–40.

44. Dai Y, Hogan S, Schmelz EM, Ju YH, Canning C, Zhou K. Selective growth inhibition of human breast cancer cells by graviola fruit extract in vitro and in vivo involving downregu-lation of EGFR expression. Nutr Cancer 2011; 63: 795–801.

45. Kroemer G, Galluzzi L, Brenner C. Mitochondrial membrane permeabilization in cell death. Physiol Rev 2007; 87: 99–163.

46. Amaral JD, Xavier JM, Steer CJ, Rodrigues CM. The role of p53 in apoptosis. Discovery Med 2010; 9: 145–52.